Journal Pre-proof

Seasonal and spatial variability of vertical particle flux along the Beagle Channel (Southern Patagonia)

X. Flores-Melo, R. Giesecke, I.R. Schloss, M.P. Latorre, X. Durrieu de Madron, F. Bourrin, M. Spinelli, C. Menniti, H.E. González, E. Menschel, J. Martín

Please cite this article as: X. Flores-Melo, R. Giesecke, I.R. Schloss, et al., Seasonal and spatial variability of vertical particle flux along the Beagle Channel (Southern Patagonia), *Journal of Marine Systems* (2023), https://doi.org/10.1016/j.jmarsys.2023.103913

Seasonal and spatial variability of vertical particle flux along the Beagle Channel (Southern Patagonia)

Flores-Melo, X.[1], Giesecke, R.[2,3], Schloss, I.R.[1,4,5], Latorre, M.P.[1], Durrieu de Madron, X.[6], Bourrin, F.[6], Spinelli, M.[7,8], Menniti, C.[6], González, H.E.[2,3], Menschel, E.[9], Martín, J.[1,10]

(1) Centro Austral de Investigaciones Científicas (CADIC), Consejo Nacional de Investigaciones Científicas y Técnicas (CONICET), Ushuaia, Argentina.

(2) Instituto de Ciencias Marinas y Limnológicas, Universidad Austral de Chile, Chile.

(3) Centro de Investigación en Ecosistemas Marinos de Altas Latitudes (IDEAL), Valdivia, Chile.

(4) Instituto Antártico Argentino (IAA), Buenos Aires, Argentina.

(5) Instituto de Ciencias Polares, Ambientes y Recursos Naturales, Universidad Nacional de Tierra del Fuego (ICPA-UNTDF), Argentina.

(6) Centre de Formation et de Recherche sur les Environnements Méditerranéens (CEFREM), Perpignan, Francia.

(7) Instituto de Biodiversidad y Biología Experimental y Aplicada, Universidad de Buenos Aires, Consejo Nacional de Investigaciones Científicas y Técnicas (IBBEA,UBA-CONICET), Buenos Aires, Argentina.

(8) Laboratorio de Zooplancton Marino. Departamento de Biodiversidad y Biología Experimental, Facultad de Ciencias Exactas (DBBE, FCEN-UBA), Buenos Aires, Argentina.

(9) Corporación Regional de Investigación y Desarrollo Cooperativo, Centro de Investigación en Ecosistemas de la Patagonia, CIEP.

(10) GRC Geociències Marines, Departament de Dinàmica de la Terra i de l'Oceà, Universitat de Barcelona (UB), E-08028 Barcelona, Spain.

Corresponding author: ximenaflores@conicet.gov.ar

Bernardo Houssay 200, Ushuaia, Tierra del Fuego, Argentina

Abstract

The Beagle Channel is a 300-km long passage connecting the Pacific and Atlantic Oceans at ~55° S, where glaciers and river streams meet subantarctic waters. Here we present the first evaluation of downward fluxes and composition of particulate matter in the channel. Settling particle fluxes were collected by sequential sediment traps deployed in two contrasting areas: one in the western part of the channel, corresponding to an early post-glacial environment (site A) and a second, fully deglaciated, river-dominated environment (site B) in the eastern part. In early summer, fluxes at both sites are driven by organic matter produced in spring, with peak organic carbon fluxes of 289 and 413 mg C m^{-2} d^{-1} at sites A and B, respectively (C:N ratios of 7.3 and 6.3, respectively). During winter, the fluxes of fecal pellets, particulate organic carbon (POC) and particulate nitrogen (PON) were at their minimum. At site A (integrated annual POC flux of 74 g C m^{-2} yr^{-1}), seasonality was weak and the flux was driven by ballast material (>95% of total particle flux) of glacial origin year-around, which also promotes the POC export. According to isotopic and taxonomic analyses performed at site A, the low seasonality in the organic component of the flux appears to be mainly related to autochthonous production of nano- and picophytoplankton during autumn and winter, later replaced by microphytoplankton fluxes during spring and summer. At site B, ballast material accounted for less than 60% of total mass flux and the POC flux showed a marked seasonality with a well-defined maximum after the spring phytoplankton bloom. Regarding the contribution of zooplankton, fecal pellets of appendicularians dominated at the western sector of the channel (site A) while *Munida gregaria* pellets dominated the flux at the eastern site (site B). This work is a contribution to ongoing efforts to unveil the physical and biogeochemical variables driving the biological carbon pump and the land-sea connections in this high-latitude ecosystem threatened by climate change.

1. Introduction

The ocean is responsible for ca. 50% of Earth's carbon sink, where the biological carbon pump plays a critical role in mitigating anthropogenic carbon emissions (Bourgeois et al., 2016). Atmospheric carbon sequestration and its burial in the ocean depend on the plankton food web structure, net ecosystem productivity, and land-coastal interactions among other factors, making predictions of carbon fluxes and pelagic-benthic coupling highly uncertain, particularly in coastal areas (Grebmeier and Barry, 1991; Mackenzie et al., 2004; Hu and Cai, 2011; Laruelle et al., 2014).

Sediment trap studies have provided critical insights on particulate organic carbon (POC) sequestration and its impact on the biogeochemical cycles of coastal and open oceans (e.g. Martín et al., 2006, 2011; Miquel et al., 2015, Gloege et al., 2017; Omand et al., 2020; Genin et al., 2021). These tools allow to characterize the composition and variability of particle fluxes in the sea, and provide critical information on both pelagic-benthic coupling as well as on the seasonal dynamics of phytoplankton and zooplankton communities (Lee et al., 1988; Buesseler et al., 2007; Lalande et al., 2020). As part of the POC, zooplankton fecal pellets are an important but highly-variable component of carbon export to depth. Different zooplankton organisms produce different types and sizes of fecal pellets, with different sinking rates (Giesecke et al., 2010; Manno et al., 2015; Turner, 2015; Cavan et al. 2017). In addition, the particulate ballast matter (BM), defined as the components collected on sediment traps that remain after combustion (450°C for 4 hours), further contributes to this flux. BM includes biogenic and lithogenic amorphous silica forms, calcium carbonate, and other inorganic compounds derived from land erosion (i.e. silts and clays) (Sarmiento, 2013). When BM is associated with organic matter (such as phytodetritus aggregates or fecal pellets), it can increase its sedimentation rate and promote a highly efficient sequestration of organic matter (Armstrong et al., 2002; Klaas and Archer, 2002; Sarmiento, 2013). In this sense, the Beagle Channel (BC) is an ideal place to study these processes. It is characterized by a strong seasonality of phytoplankton biomass (Almandoz et al., 2011; Flores-Melo et al., 2020; Iachetti et al., 2021). It is also highly compartmentalized in sub-basins with distinct physicochemical properties (Giesecke et al., 2021), and displays a marked west to east salinity gradient (Barrera et al., 2017) from glacial to riverine freshwater discharge inputs.

The Beagle Channel (Figure 1) is a complex glacio-tectonic system comprising fjords and drowned valleys which, under present sea level conditions, connects the Pacific and Atlantic Oceans at approximately 55°S (Bujalesky, 2011; Giesecke et al., 2021). The channel is delimited by several bathymetric discontinuities. In our study area, from W to E, a first bathymetric constriction is located south of Ushuaia Peninsula, where the Bridges Islands and small islets limit the eastwards along-channel circulation (Cucco et al., 2022; Martín et al., 2023). The western sub-basin of the Beagle Channel is linked to the Cordillera de Darwin Icefield, where several glaciers and fjords discharge freshwater which carries high loads of fine sediment into the channel, the so-called glacial flour (Flores et al., 2022). Eastwards from Yendegaia Fiord, the main freshwater influx to the channel originates from rivers and continental runoff (Iturraspe et al., 1989; Isla et al., 1999). The western sub-basins are deeper (~300 m) than those in the eastern sector (up to 200 m depth).

Previous studies have documented a marked seasonality of phytoplankton biomass at the eastern sub-basin of the Beagle Channel, with peaks during spring (September and October, >9 µg Chl-a L^{-1}) and low values (<0.5 µg Chl-a L^{-1}) in fall and winter, with high interannual variability (Almandoz et al., 2011). Spring and summer blooms are usually dominated by diatoms (*Chaetoceros* spp. and *Thalassiosira* spp.), while during post-bloom conditions there is a prevalence of small phytoflagellates, dinoflagellates and other members of the nano- and picoplankton (Almandoz et al., 2011; Rodríguez-Flórez et al., 2023). However, the seasonality and spatial heterogeneity of carbon export of biogenic and abiotic particle fluxes is at present unknown.

This work examines the vertical fluxes of POC and total mass by comparing sub-basins in the Beagle Channel and evaluating the potential role of ballast matter on the pelagic-benthic coupling. To achieve this, we analyze data obtained from sediment traps deployed in the study area, and consider five main variables to describe the downward particulate fluxes at each site: particulate organic matter (POM): particulate organic carbon (POC) and nitrogen (PON), the contribution of fecal pellets carbon (FPC), diatoms cells and ballast/lithogenic material (BM). For this purpose, two moorings equipped with sediment traps were deployed at two sites (A and B, Figure 1). Both sites are separated by the bathymetric barrier of the Bridges Islands (Figure 1 and Table 1).
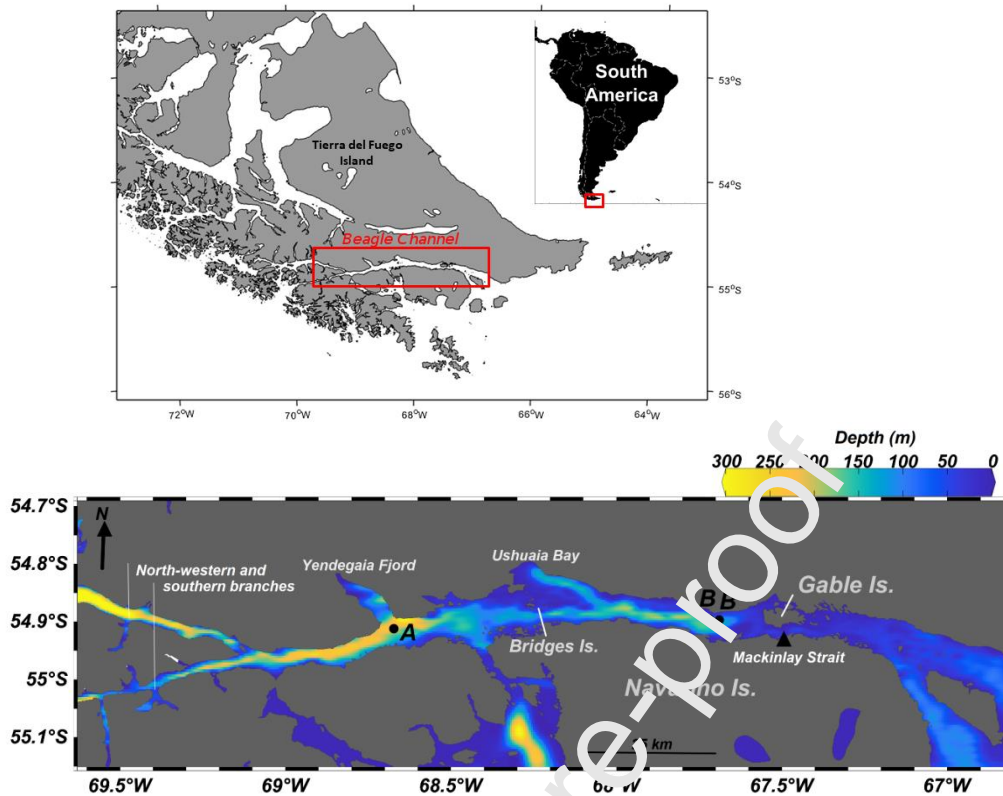
Figure 1. Study area showing the geographic position of the Beagle Channel (top) and sediment trap sampling stations (bottom): (A) The annual deployment with 15-day periodicity of a sediment trap placed in front of the entrance to Yendegaia Fjord, western sub-basin of the channel; (B) The seasonal deployment, with a 10- to 15-day sampling frequency in the eastern channel and (B'), in the same place as (B), with a 3-day deployment and a 12-hour sampling frequency.

2. Materials and Methods

2.1 Sediment trap deployments

Sequential sediment traps were used at 3 locations along the Beagle Channel (Figure 1). All three sediment traps used were Technicap cylindro-conical PPS3 traps with a collecting surface of 0.125 m^2 (Heussner et al., 1990) (For details see Table 1). From west to east: site A was located in front of the entrance to Yendegaia Fjord, while site B was near Paraná Cape. These trap deployments were set to sample the entire annual cycle. However, this continuity was feasible at site A only, as logistical difficulties resulted in fragmented sampling at site B. During the first binational survey in

November 2019, a short-term (3-days) high-frequency (12-h) sampling trap was deployed slightly offshore from site B, at site B'.

Table 1. Sampling dates and frequency, and other metadata for sediment traps deployed in the Beagle Channel. Analyses performed on sediment trap samples are also indicated. TM=Total particulate matter; POC=Particulate organic carbon; PON= Particulate organic nitrogen; BM= Ballast material; FPC= carbon associated to zooplankton fecal pellets.

	A	B	B'
Sampling dates	21/07/2017 - 16/07/2018	29/11/2015 - 12/12/2015 17/12/2015 - 9/02/2016 15/05/2016 - 13/08/2016	9/11/2019-12/11/2019
Sampling frequency (days)	15	1st period - 7 2nd period - 9 3rd period - 15	0.5
Sediment trap depth (m)	200	50	100
Number of samples	24	6	6
Bottom depth (z)	260	40	160
Latitude (ºS) **Longitude (ºW)**	54.907 68.064	54.889 67.666	54.897 67.760
Sampled variables	TM, POC, PON, BM, FPC $\delta^{13}C$, $\delta^{15}N$ diatom cell counts, Opal	TM, POC, PON, BM, FPC	TM, POC, PON, BM, FPC
Preservation agent	hypersaline NaCl–seawater (38-40 g kg^{-1}) with 1% v/v HgCl$_2$	5% (v/v) buffered formalin (e. g. Martin et al., 2006)	5% (v/v) buffered formalin (e. g. Martin et al., 2006)
Sub-samples acidification	0.2 mL of 2 N HCl	1M H$_3$PO$_4$ and 2M HCl	0.2 mL of 2 N HCl

2.2 Sample analyses

After retrieval, each sediment trap sample was filtered through a 1 mm nylon mesh in order to remove zooplankton that could have entered the traps by their own mobility and thus did not form part of the passive downward flux (e.g., Pagès et al., 2007). Each sample was fractionated to obtain subsamples with a reduced amount of material that could be retained on a GF/F filter. A number of subsamples were filtered through Whatman GF/F filters (0.7 μm pore size), previously combusted and weighted, according to Aminot and Kérouel (2004).

Filtered subsamples were dried for 12 hours at 60°C to obtain the total sample dry weight (DW, hereafter referred to as total particulate matter, TM). The same filters+samples were then combusted at 450°C for 4h to determine the ash free dry weight (hereafter referred to as ballast matter, BM). The difference between DW and BM was used to determine the organic matter (OM) weight, according to Bodungen et al. (1991).

Width, length and shape of zooplankton fecal pellets were determined using a Zeiss SV 8 stereomicroscope or an Olympus BH2 optical microscope, and then transformed into volume and carbon content according to González and Smetacek (1994) and González et al. (2000). Size and shape of the fecal pellets enabled to categorize them as belonging to appendicularians, *Munida gregaria*, copepoda, or euphausiids. Broken or non-recognizable fecal pellets were labeled "undetermined" (Alder and Morales, 2009).

Certain procedures were applied to one of the traps only, as follows:

Trap A subsamples: particulate organic nitrogen (PON) and carbon (POC) as well as their isotopic compositions were obtained from samples extracted from each collecting cup and filtered through a pre-combusted GFF filter. Samples were dried (12 h, 60 °C) and acidified with 0.2 mL of 2 N HCl to remove particulate inorganic carbon from total particulate carbon (TC), and washed with distilled water to remove excess acid. Samples were then dried at 60 °C and sent to UC Davis Stable Isotope Facility for elemental and isotopic analysis. Biogenic opal was estimated following the alkaline extraction procedure described by Mortlock and Froelich (1989) and modified by Müller and Schneider (1993). Phytoplankton identification and cell count were conducted in a 100-200 μL aliquot, following the methodology proposed by Utermöhl (1958). The small volume used is explained by the large amount of BM in the sample.

Trap B subsamples: POC and PON were measured using a VarioMAX CN, Elemental analyser (Langenselbold, Germany). Dry filtered samples were decarbonated with

repeated additions of 1M H_3PO_4 and 2M HCl until the end of effervescence (that is, the volume required to humidify the filter sample) so as to remove inorganic carbon from the sample.

Particle fluxes were calculated as:

Flux (mg m^{-2} d^{-1}) = Sample dry weight (mg) / (collecting area (m^2) / sampling interval (d)

The attenuation of POC fluxes proposed by Martin et al. (1987), adapted from Nguyen et al. (2022), was applied to estimate the potential carbon flux at a depth of 100 m (f100) as:

$$f30 = f100 \ (z \ / \ 100) \ ^{-b} \quad (Equation \ 1),$$

where $f30$ = 220 mg C m^{-2} d^{-1}, corresponding to the POC flux measured in November at a depth of z = 30 m, where b = 0.858 and refers to the attenuation coefficient proposed by Berelson (2001), and where $f100$ is the POC flux at 100 m depth.

3. Results

3.1 Downward particle fluxes at site A, western sub-basin, Yendegaia sector

The vertical fluxes measured at 200 m depth did not follow a marked seasonal pattern, although some differences between seasons can be highlighted (Figure 2). Peak POC fluxes occurred in three pulses: late spring (November), mid-summer (January) and late fall (May-June), reaching values around 270 - 300 mg C m^{-2} d^{-1} (Figure 2a). Minimum POC fluxes were observed during winter with values below 150 mg C m^{-2} d^{-1}. The contribution of POC to the total particulate flux oscillated between 1.8% in winter and maxima of 4.6 - 4.8% in spring and summer (Figure 2a). The same trends were observed by PON fluxes, with highest fluxes between 33 - 39 mg N m^{-2} d^{-1} during spring, and lowest <20 mg N m^{-2} d^{-1} during winter (Figure 2b). C:N atomic ratios ranged from 7.3 to 11.3 with minimum values in spring and maximum values in late summer (Figure 2c). During late winter, when a low C:N ratio was observed, the ballast proportion increased to 95% (Figure 2d). Highest fluxes of BM increased progressively from late summer towards the end of fall, reaching 11,554 mg m^{-2} d^{-1}. Minimum BM content (86%) and minimum BM flux occurred during mid-spring (3,840 mg m^{-2} d^{-1}).

These BM minima were simultaneous to the lowest C:N ratio in mid-spring (7.3; Figure 2d). The resulting TM flux:BM flux ratio was almost 1:1 with an $R^2 = 0.99$, indicating a predominance of BM flux (85 - 95% of the total flux; Figures 2c, d).
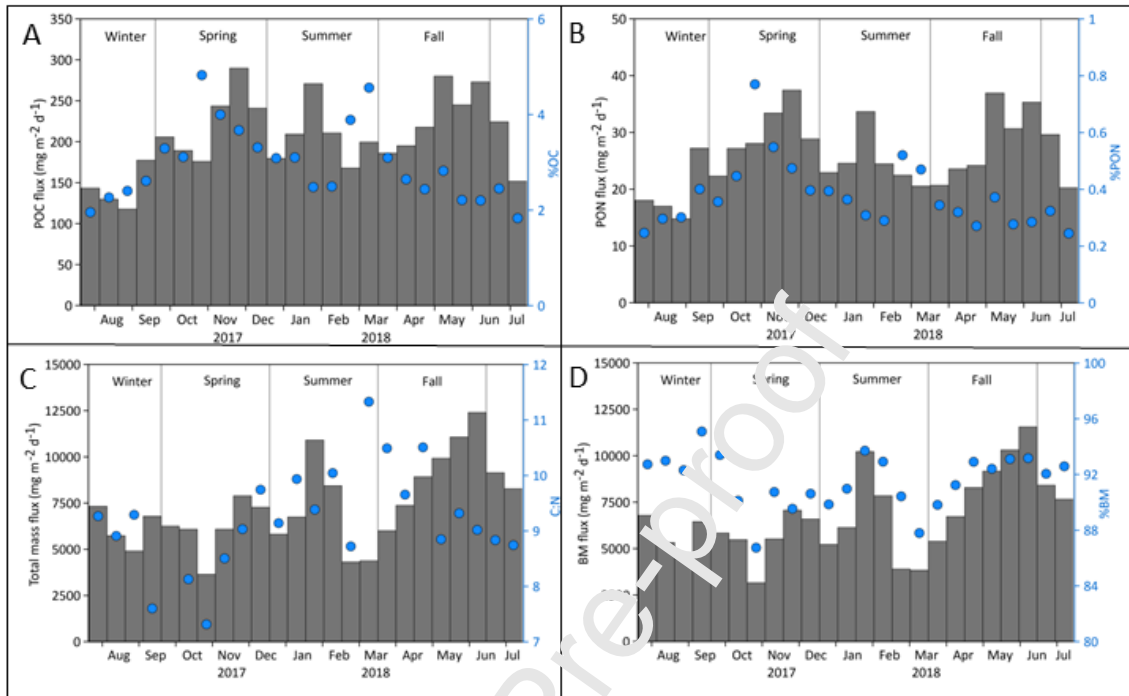

Figure 2. Magnitudes and composition of the vertical particle flux in the Beagle Channel, at sampling site A (see Figure 1 for location). (A), Particulate organic carbon (POC) fluxes (bars) and POC content as percentage of total mass (dots). (B), Particulate organic nitrogen (PON) fluxes (bars) and PON percentage of total mass (dots). (C), Total mass flux (bars) and C:N ratio (dots). (D) Ballast matter flux and percentage of total mass (dots).

Table 2. Summary of particulate matter downward fluxes and composition (% of dry weight) at the three sampled stations in the Beagle Channel (see Figure 1 for locations). TM: total mass; POC: Particulate organic carbon; PON: Particulate organic nitrogen; BM: ballast material; C:N: atomic organic carbon to nitrogen ratio. Stdv: standard deviation. Site B: Mean ± Stdv are omitted due to long periods without data.

	A (Min-Max) Mean± Stdv	B (Min-Max) Mean ± Stdv	B' (Min-Max) Mean ± Stdv
TM mg m^{-2} d^{-1}	(3646-12400) 7321 ± 2248	(204 - 3125) -	(357 - 574) 490 ± 81
POC mg m^{-2} d^{-1}	(118 - 290) 205 ± 47	(29 - 414) -	(80 - 108) 96 ± 12
PON mg m^{-2} d^{-1}	(15 - 37) 26 ± 6	(4.1 - 72.0) -	(0.9 - 1.6) 1.2 ± 0.2
BM mg m^{-2} d^{-1}	(3162-11555) 6728 ± 2146	(150 - 2751) -	(280 - 467) 396 ± 71
Opal mg m^{-2} d^{-1}	(106 – 394 241 ± 93	- -	- -
POC %	(2 - 5) 3.0 ± 0.8	(4 - 30)	(18 - 22) 20 ± 1.7
PON %	(0.2 - 0.8) 0.4 ± 0.1	(0.4 - 5.2)	(0.2 - 0.3) 0.2 ± 0.04
BM %	(87 - 95) 92 ± 2	(51 - 88)	(78 - 83) 81 ± 1.5
C:N	(7 - 11) 9.0 ± 0.9	(6.3 - 10.0)	(6.3 - 9.5) 7.8 ± 1.3

Zooplankton fecal pellet fluxes at Site A

FPC had three peaks, one at the end of spring with 157 mg C m^{-2} d^{-1}, a second in mid-summer with 152 mg C m^{-2} d^{-1} and the third at the end of the fall, with 104 mg C m^{-2} d^{-1} (Figure 3a). The spring maximum was mainly composed by fecal pellets of *M. gregaria* (96 mg C m^{-2} d^{-1}) and appendicularians (37 mg C m^{-2} d^{-1}). The summer maximum was explained by fecal pellets of euphausiids (79 mg C m^{-2} d^{-1}) and appendicularians (33 mg C m^{-2} d^{-1}), while maximum fluxes in fall were primarily linked to fecal pellets of appendicularians (35 mg C m^{-2} d^{-1}). FPC fluxes decreased during winter, reaching their minimum values (14 mg C m^{-2} d^{-1}).

Table 3. Summary of fecal pellet carbon fluxes (mg C m^{-2} d^{-1}) collected in sediment traps deployed in the Beagle Channel. Means ± Stdv at site B are omitted due to incomplete sampling.

Site	Undetermined mg C m⁻² d⁻¹	Copepods mg C m⁻² d⁻¹	Appendicularians mg C m⁻² d⁻¹	Euphausiids mg C m⁻² d⁻¹	M. gregaria mg C m⁻² d⁻¹	Total FPC mg C m⁻² d⁻¹
A						
Min-Max	2 - 57	0.3 - 11	3.5 – 104	0 - 80	0 - 96	14 - 158
Mean ± Stdv	22 ± 15	3 ± 2.5	22 ± 21	13 ±18	10 ±20	70 ± 36
B						
Min-Max	0.5 - 130	3.2 - 50	0 - 29	0.9 - 18	3.4 - 88	11 - 265
Mean ± Stdv	-	-	-	-	-	-
B'						
Min-Max	1.5 - 9.1	3.3 - 32	17 - 53	0 - 10	0 - 26	44 - 117
Mean ± Stdv	6 ± 3	9.6 ± 11	30 ± 12	1.6 ± 4	6 ± 10	81 ± 27

Considering annual year round results, integrated values of carbon export from FPC were mainly attributable to appendicularians (8 g C m⁻² y⁻¹) while 8 g C m⁻² y⁻¹ were attributable to undetermined organisms. Other well represented groups were euphausiids (4 g C m⁻² y⁻¹), *M. gregaria* (3 g C m⁻² y⁻¹) and copepods (1 g C m⁻² y⁻¹) (Table 3). Total FPC was related to total POC export (R^2 = 0.77; N = 18), accounting for 41% of annual POC fluxes and 10% of the annual TM fluxes.

Table 4. Time-averaged annual downward fluxes (g m⁻² yr⁻¹) collected in sediment trap A (See Figure 1 for location) deployed in the Beagle Channel.

	A (g m⁻² y⁻¹)
Appendicularians	8
Euphausiids	4.5
Copepods	1.. cuan
M. gregaria	3.6
Undetermined	8
total FPC	25.4
POC	73.8
PON	9.3

Opal	83.3
BM	2422
TM	2635

Phytoplankton flux at Site A

The highest opal (biogenic silica) fluxes occurred in spring and summer (October to January) and exceeded 250 mg m^{-2} d^{-1}, linked with diatom cell fluxes ($>8\times10^8$ cells m^{-2} d^{-1}) mainly composed by *Chaetoceros* spp. (65-95%), small centric diatoms (<10 μm) and *Asterionellopsis* spp. (7% in January; Figures 3b, 3c and 3d). This period was also accompanied by an increase of FPC fluxes (>120 mg C m^{-2} d^{-1}). During October, a massive diatom flux (5.9×10^9 cells m^{-2} d^{-1}) of *Chaetoceros* spp. was recorded, measuring four times the January peak (1.4×10^9 cells m^{-2} d^{-1}) and fifteen times the fall peak flux in April (0.4×10^9 cells m^{-2} d^{-1}). This massive flux was not followed by a corresponding increase in opal: despite the fact that the highest opal values (394 mg opal m^{-2} d^{-1}) were recorded during October they were only slightly higher than the following month. In late fall, a progressive but slight increase in FPC and opal fluxes (265 mg m^{-2} d^{-1}) was observed, mediated by the slight increase in diatom fluxes (3.9×10^8 cells m^{-2} d^{-1}) composed of small centric diatoms (51%) and *Chaetoceros* sp (47%).
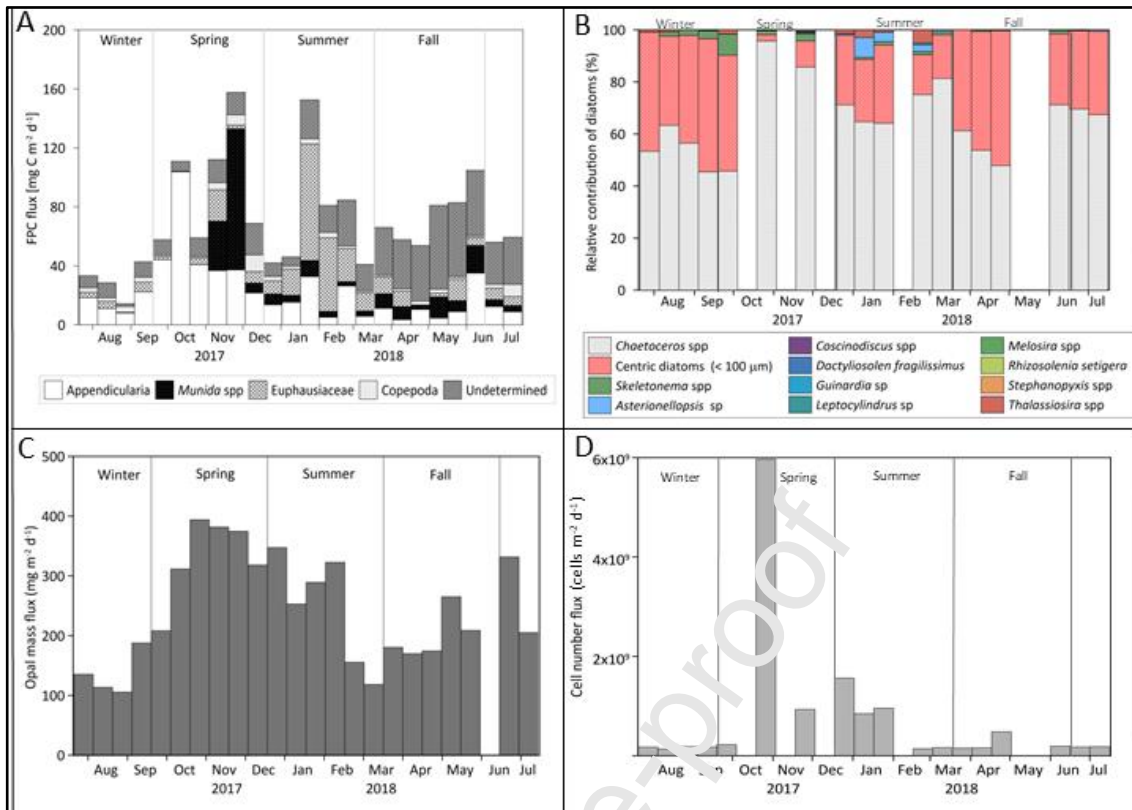
Figure 3. Particle downward fluxes at site A in the Beagle Channel (see Figure 1 for location). (A), Zooplankton fecal pellet carbon (FPC) fluxes separated by taxa. (B), relative contribution of diatom cell numbers by taxa. (C), Opal flux (mg m^{-2} d^{-1}). (D), diatom cell flux (cells m^{-2} d^{-1}).

Carbon and nitrogen isotopic ratio

The isotopic signal of the sinking particles collected at site A revealed a narrow range of values: $\delta^{13}C$ between -20 and -22.3 ‰ and $\delta^{15}N$ between 5.5 and 9.6‰ (Figure 4). $\delta^{15}N$ increased from lowest values in September-November (5.5‰ - 7.7‰) to a range of 8.6 - 9.6‰ in March-April. The lowest C:N ratio values (7.3 - 8.5) were found in spring (September to November), while maximum C:N values occurred during fall, in March-April (9.7 - 11.3).
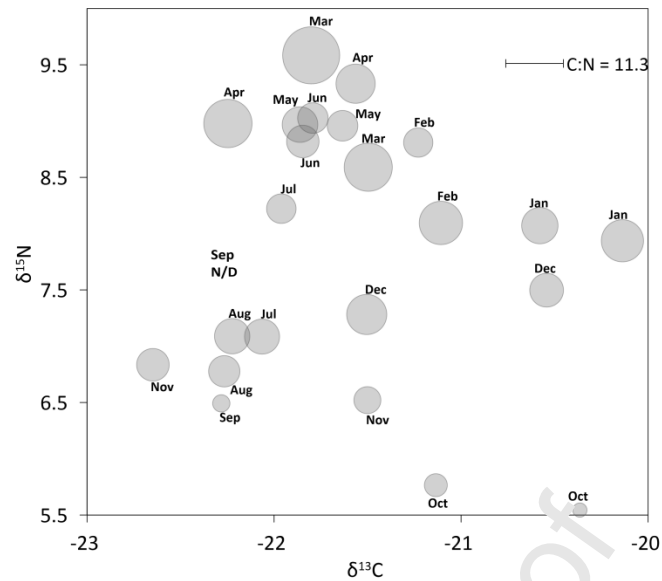
Figure 4. Carbon and nitrogen isotopic composition in sediment trap samples (each integrating 15-day intervals) at Site A (see Figure 1 for location) along an annual cycle (July 2017 - July 2018). Diameter of the circles is proportional to the C:N atomic ratio (scale shown in top right corner). N/D: no data.

3.2 Downward particle fluxes at Site B - Eastern sub-basin, Paraná Cape

Particle downward fluxes and composition at site B are shown in Figure 5. Due to technical problems and logistic difficulties, trap B was out of service for several months before it could be redeployed at the same location, resulting in an incomplete annual sampling cycle. In spite of this, a seasonal pattern of particle flux is clear at site B. Two peaks of POC and PON fluxes were observed in late spring (220.9 mg C m^{-2} d^{-1} and 72 mg N m^{-2} d^{-1}) and early summer (mid-December, 413.9 mg C m^{-2} d^{-1}; 34 mg N m^{-2} d^{-1}), with C:N ratios of 7.9 and 6.6, respectively (Figures 5a, 5b and 5c). In particular, the early summer maximum flux consisted of a perceptible (to the naked eye) amount of biogenic fresh material, with a POC content as high as 35%. After the December flux maximum, POC fluxes and content declined towards mid- summer with fluxes around 200 mg C m^{-2}d^{-1}, contributing to ca. 10% of the total flux, and reaching minimum values (41 mg C m^{-2} d^{-1}) at the end of the summer. During the sampled period in summer, C:N presented high variability, ranging between 6.3 and 10.17 over 27 days (from January 4 to February 9 2015). BM flux reached its highest values in November 2015 (2,315 mg m^{-2} d^{-1}) and January 2016 (2,751 mg m^{-2} d^{-1}; Figure 5d).
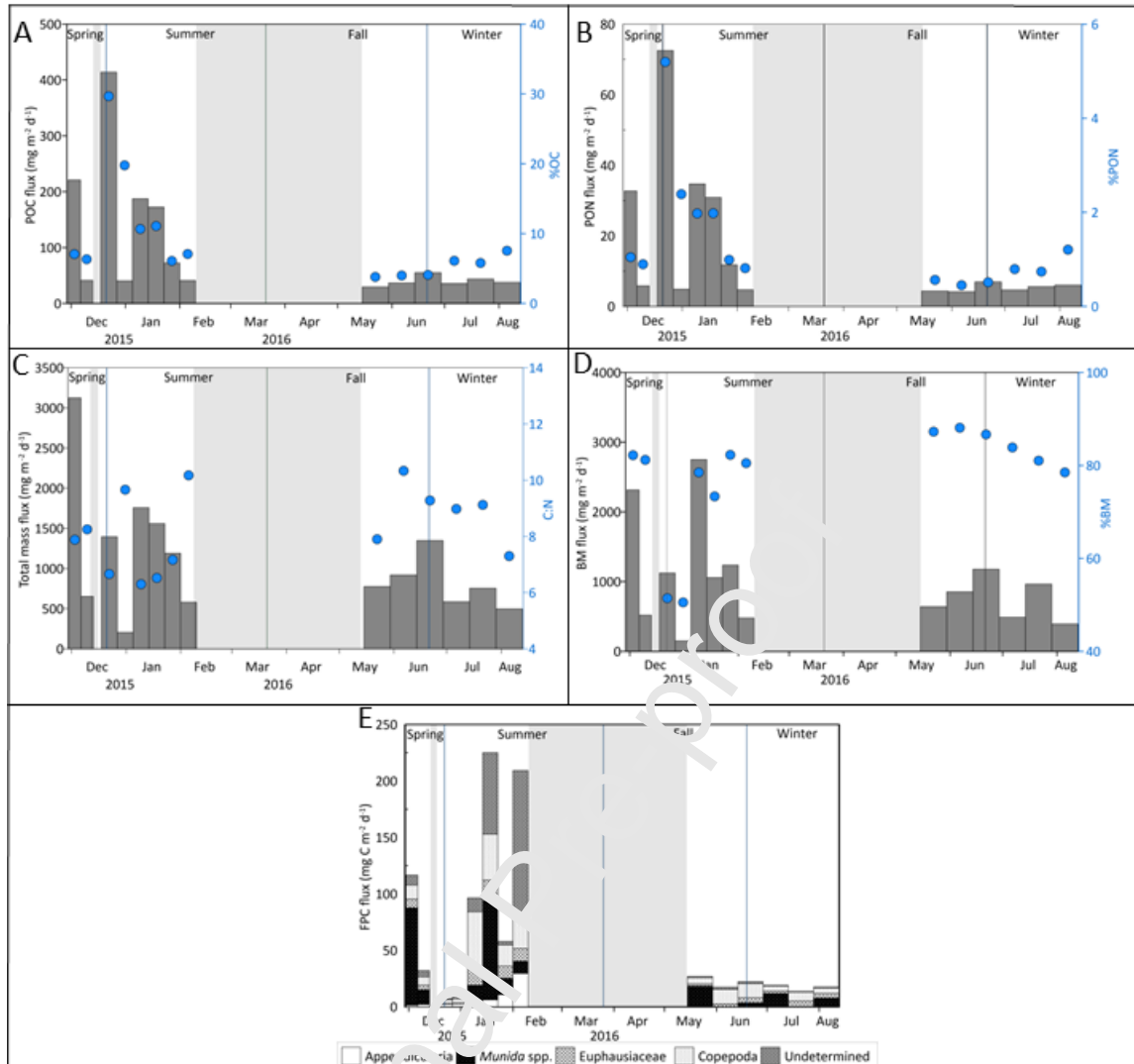
Figure 5. Particle downward fluxes and composition at site B in the Beagle Channel (see Figure 1 for location). (A) Particulate organic carbon (POC) flux (bars) and percentage of POC to total mass (dots). (B) Particulate organic nitrogen (PON) (bars) and percent of PON to total mass (dots). (C), Total mass flux (bars) and C:N ratio (dots). (D) Ballast matter (BM) flux (bars) and % BM to total mass (dots). (E) Zooplankton fecal pellets carbon (FPC) fluxes of different taxa (bars). Shaded areas indicate periods with no data owing to technical issues.

Fecal pellet flux, site B

The contribution of fecal pellets to the carbon flux displayed one peak in late spring (128.9 mg C m^{-2} d^{-1}) and several export pulses in summer, when the highest values were recorded (265.3 and 236.3 mg C m^{-2} d^{-1}) (Figure 5e). In the spring maximum (November) and the first summer maximum (January), *M. gregaria* was the main

contributor to the total carbon flux (86.4 and 87.9 mg C m^{-2} d^{-1}, respectively), followed by copepods (12.2 and 40.5 mg C m^{-2} d^{-1}) and euphausiids (7.7 and 18.2 mg C m^{-2} d^{-1}). The peak in FPC in February was composed primarily of undetermined pellets, followed by appendicularian pellets (29.5 mg C m^{-2} d^{-1}) and copepod pellets (27 mg C m^{-2} d^{-1}).

3.3 Downward particle fluxes at site B', the short-term high-temporal sampling frequency

This short-term, high-frequency trap deployment yielded a relatively low variability of POC fluxes that ranged between 79.9 and 108.34 mg C m^{-2} d^{-1} (Figure 6 and Table 2). The C:N ratio fluctuated between 6.2 and 9.5, similar to those observed in trap B (Figure 5c and 6c). During the sampling period, *M. gregaria* was the main contributor to the total FPC flux (30.8%), followed by undetermined (28%), copepods (24%), euphausiids (10.3%) and appendicularians (6.8%)

When estimated over 100 m of water column, the C flux in trap B is f100 = 78 mg C m^{-2} d^{-1} (Equation 1). This result is slightly lower but comparable to the range of POC fluxes recorded in sediment trap B' (79 - 108 mg C m^{-2} d^{-1}) in November 2019 at 100 m depth, below the pycnocline (Figure 5a).
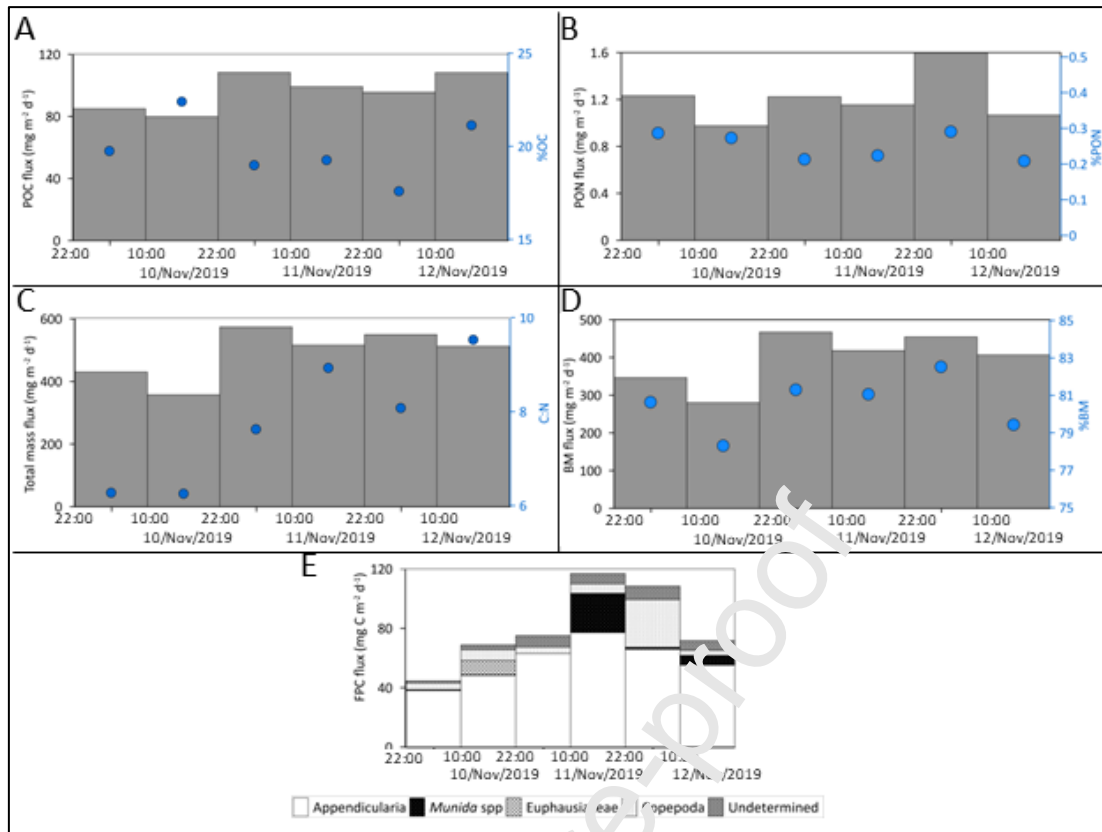
Figure 6. Particle downward fluxes at site B′ at the Beagle Channel during November 2019 (see Figure 1 for location). (A), Particulate organic carbon (POC) fluxes (bars) and percentage of POC to total mass flux (dots). (B), Particulate organic nitrogen (PON) fluxes (bars) and percentage of PON to total mass flux (dots). (C), Total mass (TM) flux (bars) and C:N molar ratio (dots). (D), fecal pellet carbon (FPC) flux of different taxa (bars).

3.4 General compositional trends

In Figure 7, ballast matter (BM) and POC fluxes obtained at the three trap sites are plotted against total mass fluxes to assess trends in the main constituents. Site A showed a relatively constant composition throughout the year with high BM content (86% - 95%) and its TM fluxes were always higher than those of site B (Figure 7). Site B showed a higher variability in BM and POC composition at all time scales presented (12 hours to 15 days), and POC contents exceeded those of site A. The contents of BM and POC tend asymptotically towards very low values in % organic carbon and 90% for ballast when total mass fluxes increase.
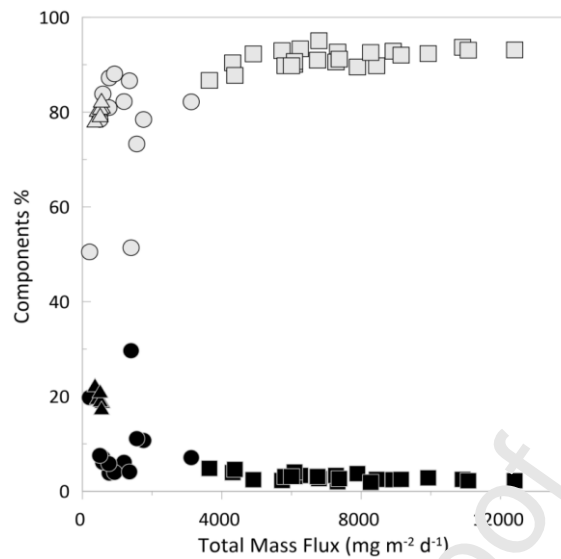
Figure 7. Percentage of particulate organic carbon (black symbols) and ballast material (light gray symbols) versus total downward particle flux in sediment trap samples from the Beagle Channel. Samples from all 3 sediment trap deployments shown in Figure 1 are merged in the figure. Squares: trap A; circles: trap B; triangles: trap B'.

4. Discussion

This work presents the first assessment of settling particle fluxes and composition in the Beagle Channel, a critically understudied high-latitude ecosystem. The three sediment traps, deployed at different locations along the channel and with different sampling schedules, provide the basis for investigating the spatio-temporal variability and the processes involved in particle export from the surface to the seafloor.

4.1. Environmental hydrological conditions

Previous studies show relatively similar trends in terms of seasonal vertical stratification at the two studied sites (Giesecke et al., 2021). Also, a decrease of sea surface density in December allows for the establishment of the summer pycnocline, increasing stratification and stability in the upper water column (Flores-Melo et al., 2020). Although the pycnocline acts as a particle retention barrier in the upper mixed layer at both sites, at site B during spring there is a strong POC flux when the pycnocline starts

to form. During summer, when the pycnocline is well established, small POC fluxes continue and can be linked to small BM and pellet fluxes: this is known to enhance the vertical flux of carbon despite stratification. Regarding the local production and flux of organic matter, in site A the proliferation of autotrophic organisms is limited by BM-driven light attenuation. In contrast, at site B the proliferation of photosynthetic organisms further contributes to POC fluxes, since light limitation is minor (Schloss et al., 2023).

4.2. On the composition, magnitude and seasonality of particle fluxes

The annual carbon flux recorded at site A (73.8 g C m^{-2} yr^{-1}, Table 4) is comparable to the lower limit of annual export recorded in a similar high-latitude system such as the Kobbefjord in West Greenland (76-106 g C m^{-2} yr^{-1}; Sejr et al., 2014), but is twice the maximum annual flux recorded in Shelikof Strait (Alaska) (48.6 g C m^{-2} yr^{-1}; Rember and Trefry, 2005). These results contrast with those from a lower latitude system, the Laurentian Channel in the Gulf of St. Lawrence (48 - 49 °N), where the annual carbon flux was 1.1 g C m^{-2} yr^{-1} (Genin et al., 2021).

Despite incomplete year around sampling in the case of site B, some features are worth highlighting, namely the maxima of total and organic fluxes detected in spring-summer, which are consistent with the seasonal phytoplankton bloom known for this region (Almandoz et al., 2011). Unlike at site B, there is no obvious seasonality in the vertical POC fluxes at site A which shows higher carbon export during spring, summer and fall and a slightly lower contribution during the winter periods. This low seasonal variability might be linked to fresh water discharge loaded with mineral material of glacial origin which, when associated with organic matter, enhances its sedimentation through the seasonal pycnocline (Armstrong et al., 2002). The organic matter deposited during warmer periods corresponds to phytoplankton assemblages observed as a strong pulse of fluorescence in spring, decreasing towards summer and autumn (Flores-Melo et al., 2020). The spring pulse corresponds to microphytoplankton communities and is reflected in the decrease in the isotopic signal of δ^{13}C (range between 20.5 - 21.5‰), in line with what is expected for marine phytoplankton in this area (21 ± 0.5‰; average ± Stdev, Riccialdelli et al., 2017; Figure 5).

During the spring-summer phytoplankton production season, sites A and B displayed C:N ratios (7.3 and 6.3, respectively) as expected for marine particulate matter and implying relative N-rich and low remineralized organic matter export linked to high fluxes of new production (Copin-Montegut and Copin-Montegut, 1983; Geider and La Roche, 2002). During the fall-winter seasons in the southern Patagonia fjord ecosystems, environmental conditions (low solar radiation and vertical mixing) promote the growth of small autotrophic nano- and picoplankton that support secondary production with a food web dominated by the microbial loop (Harmelin-Vivien et al., 2008; González et al., 2013; Lutz et al., 2016; Iriarte et al., 2018; Rodríguez-Flórez et al., 2023). This change in the plankton community structure leads to changes in the biological carbon pump intensity but allows for the sustainability of labile organic matter during fall and winter (Legendre and Le Fevre, 1995). At site B, the maximum carbon flux (413 mg C m^{-2} d^{-1}) was related to a diatom bloom dominated almost exclusively by *Guinardia delicatula,* a common marine species in both this sub-basin of the Beagle Channel during spring and summer (Almandoz et al., 2019) as well as in northern Patagonian fjords (González et al. 2013). No massive fluxes of *G. delicatula* were recorded at site A where this diatom contributed just 0.015% of the relative cell abundance during the entire sampling period (max. contribution 0.2% on 18-11-2017, data not shown).

The sub-basin of site B is under direct anthropogenic pressure from the growing population of Almanza, Puerto Williams and the city of Ushuaia. It is possible that high nutrient loads from a submarine emissary of the Ushuaia sewage plant (Golondrina Bay) may fuel increased nutrients (i.e., ammonia), while silicic acid may be available from resuspended sediments favoring *G. delicatula* massive blooms in site B (Diodato et al., 2020; Giesecke et al., 2021). In contrast, no human settlements exist in the vicinity of the site A sub-basin, which explains the more pristine conditions that prevail there. This finding highlights the important role of species that are not usually widely dominant in producing massive carbon exports and CO_2 sinks over very short periods, thus boosting benthic communities through the export of labile organic matter with a low C:N ratio.

The diatom community of site A was instead dominated in mid-spring by centric diatoms of the genus *Chaetoceros* spp. (Figures 3b, 3c and 3d), a common genus in fjords and channels throughout Patagonia, showing highest abundances in spring-

summer (Alves-de-Souza et al., 2008; Almandoz et al., 2011). Several cold-water *Chaetoceros* species have been shown to dominate under low nutrient concentrations (Booth et al., 2002; Tas and Hernández-Becerril, 2017): this is likely related to the intermediate surface to volume ratio (S/V ~1μm^{-1}) of these cells, which would explain the dominance of *Chaetoceros* spp. throughout the year (Alves-de-Souza et al., 2008). Some species in this genus might also have particularly low silicate demands, such as those belonging to the hyalochaeta group (Varela et al., 2004). A massive flux of this genus has only been recorded once (during October 2017), highlighting the conspicuous blooming of phytoplankton in this region which is greatly limited both in light and in macronutrients (nitrate and silicic acid; Cuevas et al., 201?; Giesecke et al., 2021). Carbon flux related to diatom communities accounts for a minor fraction of the total organic carbon fluxes of the sediment trap at site A; it is thus more likely that the nano-picoplankton community plays a major role in the carbon fluxes in this region. This community is usually overlooked due to its small size and the absence of conspicuous structures, which prevents them from being easily identified from sediment trap samples. Nano- and picoplankton are the main components of the autotrophic community during the austral winter and are a remarkable phytoplankton carbon source in this high latitude ecosystem (Paredes and Montecino, 2011; Rodríguez-Flórez et al., 2023). These organisms are capable of growing to achieve high biomass under low nutrient concentrations due to their high surface to volume ratio as well as to their efficient capture of photons, a clear advantage when light is a limiting factor (Sunda and Huntsman, 1997) as is the case in southern Patagonia (Cuevas et al., 2019).

When small centric diatoms (<20 μm) dominate phytoplankton assemblages, the role of appendicularians in carbon export via fecal pellets is noteworthy, considering that, together with "undetermined" fecal pellets, they were the main group contributing to the integrated annual export of carbon in the form of pellets at site A. These filter-feeding organisms prey mainly on the nano- and picoplanktonic fraction (Bedo et al., 1993; Fernández et al., 2004), consisting most likely of appendicularians as well as small copepod species (i.e. *Oithona* spp.) that are the main pathways to the carbon transport along the food web (Giesecke et al., 2019). During spring and summer blooms, when microphytoplankton tend to dominate, *M. gregaria* plays an important role in the pelagic-benthic coupling by the production of large (260±194 mm^3) and rapidly (700 - 1200 m d^{-1}) sinking fecal pellets (Giesecke, unpublished). This species is one of the

most abundant macroplanktonic crustaceans in Argentinian continental shelf waters (Dellatorre et al., 2008) and Chilean Patagonian fjords (Meerhof et al., 2013) and is an opportunistic feeder, exhibiting cannibalism, scavenging and filter feeding behaviors (Pérez-Barros et al., 2010). In the Beagle Channel, *M. gregaria* is present year around in similar abundances, with larval stages more prevalent in spring and summer (Lovrich, 1999; Diez et al., 2018).

The total carbon exported as FPC at site A was about 2.4 times higher than at site B. Euphausiid and appendicularian FPC showed peak carbon fluxes 7 and 9 times higher at site A than at site B, respectively. However, the maximum carbon flux associated to copepod fecal pellets was six times higher at site B than at site A, even when the discontinuous data in the latter are taken into consideration, while FPC of *M. gregaria* registered similar maximum carbon flux values at both sites (Table 3).

4.3. Origin of settling particles

In site A, the inputs of terrestrial particulate lithogenic matter during pulses along the year lead the TM flux and act as ballast material. These sedimentation pulses took place during summer and fall. The isotopic range of the particles sequestered by the traps (δ^{13}C between -20 and -26‰; δ^{15}N between 5.5 and 9.5‰) supports the hypothesis that the planktonic food web is nourished by marine phytoplankton and that carbon is transported to the seafloor agglutinated with BM and fecal pellets. Such isotopic ranges are comparable to those found in the water column of the Argentinian South Patagonian shelf (δ^{13}C -25 to -19‰; δ^{15}N 2 to 9.5‰), but lower than those from the Northern Drake Passage (δ^{13}C -30 to -25‰; δ^{15}N -2 to <0.6‰) (Lara et al., 2010). Previous results from the Beagle Channel showed δ^{15}N values of 7.5‰ (±0.85‰) in March in suspended particulate matter, highlighting that the δ^{15}N enrichment of particulate organic matter is led by nitrate consumption by the phytoplankton community in fall (Lara et al., 2010; Cardona-Garzón et al., 2016). In turn, δ^{13}C enrichment in the Antarctic Peninsula has been linked to the predominance of nanoflagellates, increasing the range from -27 to -23‰ and supporting the suggestion that nanoplanktonic organisms are a key component in Yendegaia communities (δ^{13}C close to -23‰).

$\delta^{13}C$ enrichment increases with BM flux ($R^2 = 0.7$; N = 20), indicating that BM in the vicinity of site A plays a critical role in POC fluxes, and therefore in efficient carbon sequestration. The turbidity plumes previously described as *glacier flour* might therefore be responsible for promoting an efficient vertical carbon export in this region, contributing to enhancing the biological carbon pump in the southern Patagonia region, where intense CO_2 fluxes from the atmosphere to the ocean have been observed (Torres et al., 2011; Flores et al., 2022; Latorre et al., 2023).

4.4 Effect of ballast material on the vertical carbon export

Despite sites A and B being only 60 km apart in the middle of Beagle Channel, the fluxes measured by sediment traps at these locations were remarkably different, not only in terms of magnitude, but also when examined in the temporal evolution of POC fluxes. Site A in front the entrance to Yendegaia Fjord has a low seasonality, with relatively high fluxes year around that are strongly dominated by inorganic particles, likely *glacier flour* (Flores et al., 2022). While the highest fluxes of inorganic particles are expected to occur during the melting season (austral spring and summer), maximum fluxes in this study site were recorded in two pulses in mid-summer and at the end of fall. Unfortunately, there is no information available on the melting dynamics of the glaciers feeding the deltaic system of the Yendegaia Fjord, limiting any further discussion.

In general, organic carbon contents decreased with increasing TM fluxes, supporting the hypothesis that BM limits the proliferation of the phytoplankton community and negatively conditions the diet of zooplankton through contributions of terrigenous material (Giesecke et al., 2019). A more terrigenous and homogeneous composition of the total particulate matter occurs in periods of high fluxes (Figure 8), whatever the site and depth. A conceptual model summarizing the results presented in the discussion is shown in Figure 9.
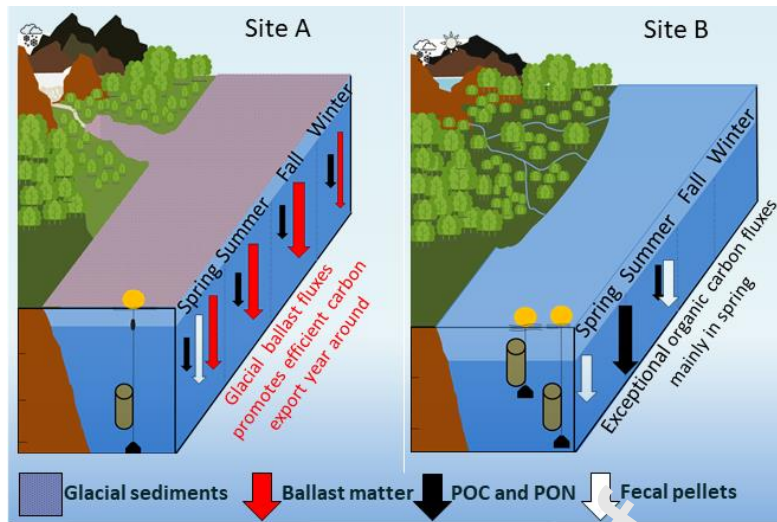
Figure 8. Conceptual model summarizing the main results obtained at the western (left) and eastern (right) sectors of the study area.

Concluding remarks

In this study we present the first results of particulate organic matter fluxes (POC, PON, plankton organisms and fecal pellets) from the Beagle Channel. We also highlight the importance of terrigenous mineral material that acts as ballast material year around. This occurs particularly in the vicinity of glacier-influenced areas such as site A where the export of marine-produced carbon toward the benthic communities is favored. Both studied sites show a seasonal pattern of stratification followed by warming, and by cooling of the surface layer starting in November. The spring microphytoplankton bloom and cell packing into dense and rapidly sinking fecal pellets by key species, as well as the ballasting of aggregates by mineral particles are shown to be key processes that explain the efficient carbon export in the Beagle Channel. The flux of microphytoplankton-derived organic matter of high nutritional value for the benthic community occurs prior to the stratification of the water column. Our results show that in the area near Yendegaia Fjord, the nano- and picoplankton community sustains carbon fluxes in fall and winter, driven by lithogenic or ballast material and fecal pellets. In site B, near Paraná Point, ballast material fluxes and fecal pellets are seen to have a lower contribution to carbon sequestration during fall/winter.

References

Alder, V.A. and Morales, C. E. (2009). Microplancton y productos zooplanctónicos. In: Manual de métodos para el estudio de sistemas marinos. (Ed. Alder, V.A and Morales C. E). Eudeba, Argentina. 272 pp.

Almandoz, G. O., Hernando, M. P., Ferreyra, G. A., Schloss, I. R., and Ferrario, M. E. (2011). Seasonal phytoplankton dynamics in extreme southern South America (Beagle Channel, Argentina). J. Sea Res. 66, 47–57. https://doi.org/10.1016/j.seares.2011.03.005

Almandoz, G.O., Cefarelli, A.O., Diodato, S., Montoya, N.G., Benavides, H.R., Carignan, M., Hernando, M., Fabro, E., Metfies, K., Lundholm, N., Schloss, I.R., Álvarez, M., Ferrario, M.E., (2019). Harmful phytoplankton in the Beagle Channel (South America) as a potential threat to aquaculture activities. Mar. Pollut. Bull. 145, 105–117. https://doi.org/10.1016/j.marpolbul.2019.05.026

Alves-de-Souza, C., González, M. T., and Iriarte, J. L. (2008). Functional groups in marine phytoplankton assemblages dominated by diatoms in fjords of southern Chile. Journal of Plankton Research, 30(11), 1233-1243. https://doi.org/10.1093/plankt/fbn079

Aminot, A., and Kérouel, R. (2004). Hydrologie des écosystèmes marins: paramètres et analyses. Editions Quae

Armstrong, R. A., Lee, C., Hedges, J. I., Honjo, S., and Wakeham, S. G. (2002). A new, mechanistic model for organic carbon fluxes in the ocean based on the quantitative association of POC with ballast minerals Deep Sea Research Part II: Topical Studies in Oceanography, 49(1-3), 219-236. https://doi.org/10.1016/S0967-0645(01)00101-1

Barrera, F., Lara, R. J., Krock, B., Garzón-Cardona, J. E., Fabro, E., & Koch, B. P. (2017). Factors influencing the characteristics and distribution or surface organic matter in the Pacific-Atlantic connection. Journal of Marine Systems, 175, 36-45. https://doi.org/10.1016/j.jmarsys.2017.07.004

Bedo, A. W., Acuna, J. L., Robins, D., and Harris, R. P. (1993). Grazing in the micron and the sub-micron particle size range: the case of Oikopleura dioica (Appendicularia). Bulletin of Marine Science, 53(1), 2-14

Berelson, W. M. (2001). Particle settling rates increase with depth in the ocean. Deep Sea Research Part II: Topical Studies in Oceanography, 49(1-3), 237-251. https://doi.org/10.1016/S0967-0645(01)00102-3

Bodungen, V. B., Wunsch, M., and Fürderer, H. (1991). Sampling and analysis of suspended and sinking particles in the northern North Atlantic. In: Marine particles: analysis and characterization. AGU Geophysical Monography 63, 47–56. https://doi.org/10.1029/GM063p0047

Booth, B. C., Larouche, P., Bélanger, S., Klein, B., Amiel, D., and Mei, Z. P. (2002). Dynamics of Chaetoceros socialis blooms in the North Water. Deep Sea Research Part II: Topical Studies in Oceanography, 49(22-23), 5003-5025. https://doi.org/10.1016/S0967-0645(02)00175-3

Bourgeois, T., Orr, J. C., Resplandy, L., Terhaar, J., Ethé, C., Gehlen, M., and Bopp, L. (2016). Coastal-ocean uptake of anthropogenic carbon. Biogeosciences, 13(14), 4167-4185. https://doi.org/10.5194/bg-13-4167-2016

Buesseler K.O., A.N. Antia, M. Chen, S.W. Fowler, W.D. Gardner, O. Gustafsson, K. Harada, A.F. Michaels, M.Rutgers van der Loeff, M. Sarin, D.K. Steinber and Thomas Trull (2007). An assessment of the use of sediment traps for estimating upper ocean particle fluxes. Journal of Marine Research, 65, 345–416. https://doi.org/10.1357/002224007781567621

Bujalesky, G. G. (2011). La inundación del Valle Beagle (11.000 AÑOS A.P.), Tierra del Fuego. The Flood of the Beagle Valley (11.000 YR B.P.), Tierra del Fuego. Anal. Inst. Patagonia, 39(1), 5–21. https://doi.org/10.4067/s0718-686x2011000100001

Cardona-Garzón, J.E., Martínez, A.M., Barrera, F., Pfaff, F., Koch, B.P., Freije, R.H., Gómez, E.A., Lara, R.J. (2016). The Pacific-Atlantic connection: Biogeochemical signals in the southern end of the Argentine shelf. J. Mar. Syst. 163, 95–101. https://doi.org/10.1016/j.jmarsys.2016.07.008

Cavan, E. L., Henson, S. A., Belcher, A., and Sanders, R. (2017). Role of zooplankton in determining the efficiency of the biological carbon pump. Biogeosciences, 14, 177–186. https://doi.org/10.5194/bg-14-177-2017

Copin-Montegut, C., and G. Copin-Montegut 1983. Stoichiometry of carbon, nitrogen, and phosphorus in marine particulate matter. Deep Sea Research Part A. Oceanographic Research Papers 30(1):31–46. https://doi.org/10.1016/0198-0149(83)90031-6

Cucco, A., Martín, J., Quattrocchi, G., Fenco, H., Umgiesser, G., Fernández, D.A. (2022). Water Circulation and Transport Time Scales in the Beagle Channel, Southernmost Tip of South America. J. Mar. Sci. Eng. 10, 941. https://doi.org/10.3390/jmse10070941

Cuevas, L. A., Tapia, F. J., Iriarte, J. L., González, H. E., Silva, N., and Vargas, C. A. (2019). Interplay between freshwater discharge and oceanic waters modulates phytoplankton size-structure in fjords and channel systems of the Chilean Patagonia. Progress in Oceanography 173, 103-113. https://doi.org/10.1016/j.pocean.2019.02.012

Dellatorre, F. G., and Baron, P. J. (2008). Multiple spawning and length of embryonic development of Munida gregaria in northern Patagonia (Argentina). Journal of the Marine Biological Association of the United Kingdom, 88(5), 975-981. https://doi.org/10.1017/S0025315408001653

Diez, M.J., Cabreira, A.G., Madirolas, A., Martín, J., Scioscia, G., Schiavini, A., Lovrich, G.A., (2018). Winter is cool: spatio-temporal patterns of the squat lobster Munida gregaria and the Fuegian sprat Sprattus fuegensis in a sub-Antarctic estuarine environment. Polar Biol. 41, 2591-2605. https://doi.org/10.1007/s00300-018-2394-2

Diodato, S., González Garraza, G., Mansilla, R., Moretto, A., Escobar, J., Méndez-López, M., Gómez-Armesto, A., Marcovecchio, J., Nóvoa-Muñoz, J.C. (2020). Quality changes of fluvial sediments impacted by urban effluents in Ushuaia, Tierra del Fuego, southernmost Patagonia. Environ. Earth Sci. 79, 1–14. https://doi.org/10.1007/s12665-020-09236-4

Fernández, D., López-Urrutia, Á., Fernández, A., Acuña, J. L., and Harris, R. (2004). Retention efficiency of 0.2 to 6 μm particles by the appendicularians Oikopleura dioica and Fritillaria borealis. Marine Ecology Progress Series, 266, 89-101. https://doi.org/10.3354/meps266089

Flores, R. P., Lara, C., Saldías, G. S., Vásquez, S. I., and Roco, A. (2022). Spatio-temporal variability of turbid freshwater plumes in the Inner Sea of Chiloé, northern Patagonia. Journal of Marine Systems, 103709. https://doi.org/10.1016/j.jmarsys.2022.103709

Geider, R., and La Roche J. 2002. Redfield revisited: Variability of C:N:P in marine microalgae and its biochemical basis. European Journal of Phycology 37(1):1–17. https://doi.org/10.1017/S0967026201003456

Genin, F., Lalande, C., Galbraith, P. S., Larouche, P., Ferreyra, G. A., and Gosselin, M. (2021). Annual cycle of biogenic carbon export in the Gulf of St. Lawrence. Continental Shelf Research, 221, 104418. https://doi.org/10.1016/j.csr.2021.104418

Giesecke, R., González, H.E. and Bathmann, U. (2010). The role of the chaetognath *Sagitta gazellae* in the vertical carbon flux of the Southern Ocean. Polar Biol 33, 293–304. https://doi.org/10.1007/s00300-009-0704-4

Giesecke, R., Höfer, J., Vallejos, T., and González, H. E. (2019). Death in southern Patagonian fjords: copepod community structure and mortality in land-and marine-terminating glacier-fjord systems. Progress in Oceanography, 174, 162 - 172. https://doi.org/10.1016/j.pocean.2018.10.011

Giesecke R, Martín J, Piñones A, Höfer J, Garcés-Vargas J, Flores-Melo X, Alarcón E, Durrieu de Madron X, Bourrin F and González, HE. (2021). General Hydrography of the Beagle Channel, a Subantarctic Interoceanic Passage at the Southern Tip of South America. Front. Mar. Sci. 8:621822. https://doi.org/10.3389/fmars.2021.621822

Gloege, L., McKinley, G. A., Mouw, C. B. and Ciochetto, A. B. Global evaluation of particulate organic carbon flux parameterizations and implications for atmospheric pCO2. (2017). Glob. Biogeochemical Cycles 31, 1192–1215. https://doi.org/10.1002/2016GB005535

González, H.E. and Smetacek, V. (1994). The possible role of the cyclopoid copepod Oithona in retarding vertical flux of zooplankton fecal material. Marine Ecology Progress Series, 113(3), 233-246. https://doi.org/10.2307/24849522

González, H.E., Ortiz, V. C., Sobarzo, M. (2000). The role of faecal material in the particulate organic carbon flux in the northern Humboldt Current, Chile (23°S), before and during the 1997–1998 El Niño. J. Plankton Res. 22, 499–529, 22: 499–529. https://doi.org/10.1093/plankt/22.3.499

González, H. E., Castro, L. R., Daneri, G., Iriarte, J. L., Silva, N., Tapia, F., Teca E., and Vargas, C. A. (2013). Land–ocean gradient in haline stratification and its effects on plankton dynamics and trophic carbon fluxes in Chilean Patagonian fjords (47–50 S). Progress in Oceanography, 119, 32-47. https://doi.org/10.1016/j.pocean.2013.06.003

Grebmeier, J. M., and Barry, J. P. (1991). The influence of oceanographic processes on pelagic-benthic coupling in polar regions: a benthic perspective. J. Mar. Syst., 2: 495-518. https://doi.org/10.1016/j.dsr2.2008.05.017

Harmelin-Vivien, M., Loizeau, V., Mellon, C., Beker, B., Arlhac, D., Bodiguel, X., Ferraton, F., Hermand, R., Philippon, X., Salen-Picard, C. (2008). Comparison of C and Nstable isotope ratios between surface particulate organic matter and microphytoplankton in the Gulf of Lions (NW Mediterranean). Cont. Shelf Res. 28, 1911–1919. https://doi.org/10.1016/j.csr.2008.03.002

Heussner, S., Ratti, C., Carbonne, J., (1990). The PPS 3 time-series sediment trap and the trap sample processing techniques used during the ECOMARGE experiment. Cont. Shelf Res. 10, 943–958. https://doi.org/10.1016/0278-4343(90)90069-X

Hu, X., and Cai, W. J. (2011). An assessment of ocean margin anaerobic processes on oceanic alkalinity budget. Global Biogeochem. Cycles, 25, GB3003. https://doi.org/10.1029/2010GB003859

Iriarte, J.L., Cuevas, L.A., Cornejo, F., Silva, N., González, H.E., Castro, L., Montero, P., Vargas, C.A., Daneri, G. (2018). Low spring primary production and microplankton carbon biomass in Sub-Antarctic Patagonian channels and fjords (50–53°S). Arctic, Antarct. Alp. Res. 50. https://doi.org/10.1080/15230430.2018.1525186

Iachetti, C. M., Lovrich, G., & Alder, V. A. (2021). Temporal variability of the physical and chemical environment, chlorophyll and diatom biomass in the euphotic zone of the Beagle Channel (Argentina): evidence of nutrient limitation. Progress in Oceanography, 195, 102576. https://doi.org/10.1016/j.pocean.2021.102576

Isla, F., Bujalesky G., and Coronato, A. (1999). Procesos estuarinos en el canal Beagle, Tierra del Fuego. Revista de la Asociación Geológica Argentina, 54(4), 307-318

Karl, D. M., and Lukas, R. (1996). The Hawaii Ocean Time-series (HOT) program: Background, rationale and field implementation. Deep Sea Research Part II: Topical Studies in Oceanography, 43(2-3), 129-156. https://doi.org/10.1016/0967-0645(96)00005-7

Laruelle, G. G., Lauerwald, R., Pfeil, B., and Regnier, P. (2014). Regionalized global budget of the CO2 exchange at the air-water interface in continental shelf seas. Global Biogeochem. Cycles, 28, 1199– 1214. https://doi.org/10.1002/2014GB004832

Lalande, C., Grebmeier, J. M., Hopcroft, R. R., and Danielson, S. L. (2020). Annual cycle of export fluxes of biogenic matter near Hanna Shoal in the northeast Chukchi Sea. Deep Sea Research Part II: Topical Studies in Oceanography, 177, 104730. https://doi.org/10.1016/j.dsr2.2020.104730

Lara, R. J., Alder, V., Franzosi, C. A., and Kattner, G. (2010). Characteristics of suspended particulate organic matter in the southwestern Atlantic: influence of temperature, nutrient and phytoplankton features on the stable isotope signature. Journal of Marine Systems, 79(1-2), 199-209. https://doi.org/10.1016/j.jmarsys.2009.09.002

Latorre, M.P., Berghoff, C.F., Giesecke, R., Malits, A., Pizarro, G., Iachetti, C.M., Martin, J., Flores-Melo, X., Gil, M.N., Iriarte, J.L.,Schloss, I.R. 2023. Plankton

metabolic balance in the eastern Beagle Channel during spring. Journal of Marine Systems, 240: 103882. https://doi.org/10.1016/j.jmarsys.2023.103882

Lee, C., Wakeham, S.G., and Hedges, J.I. (1988). The measurement of oceanic particle flux—Are "swimmers" a problem?. Oceanography 1(2):34–36

Legendre, L., Le Fevre, J. (1995). Microbial food webs and the export of biogenic carbon in oceans. Aquat. Microb. Ecol. 9, 69–77. https://doi.org/10.3354/ame009069

Lovrich, G. A. (1999). Seasonality of larvae of Brachyura and Anomura (Crustacea decapoda) in the Beagle Channel, Argentina. Scientia Marina, 63(S1), 347-354. https://doi.org/10.3989/scimar.1999.63s1347

Lutz, V., Frouin, R., Negri, R., Silva, R., Pompeu, M., Rudorff, N., Cabral, A., Dogliotti, A., Martinez, G. (2016). Bio-optical characteristics along the Straits of Magallanes. Cont. Shelf Res. 119, 56–67. https://doi.org/10.1016/j.csr.2016.03.008

Mackenzie, F. T., Lerman, A., and Andersson, A. J. (2004). Past and present of sediment and carbon biogeochemical cycling models. Biogeosciences, 1(1), 11-32. https://doi.org/10.5194/bg-1-11-2004

Manno, C., Stowasser, G., Enderlein, P., Fielding, S., and Tarling, G. A. (2015). The contribution of zooplankton faecal pellets to deep-carbon transport in the Scotia Sea (Southern Ocean), Biogeosciences, 12, 1955-1965. https://doi.org/10.5194/bg-12-1955-2015

Martin, J. H., Knauer, G. A., Karl, D. M., and Broenkow, W. W. (1987). VERTEX: carbon cycling in the northeast Pacific. Deep Sea Research Part A. Oceanographic Research Papers, 34(2), 267-285. https://doi.org/10.1016/0198-0149(87)90086-0

Martín, J., Palanques, A., Puig, P. (2006). Composition and variability of downward particulate matter fluxes in the Palamós submarine canyon (NW Mediterranean). J. Mar. Syst., 60: 75-97. https://doi.org/10.1016/j.jmarsys.2005.09.010

Martín, J., Palanques, A. Vitorino, J., Oliveira, A., de Stigter, H. (2011). Near-bottom particulate matter dynamics in the Nazaré submarine canyon under calm and stormy conditions. Deep-Sea Research II, 58 (23-24)

Martín, J., Alonso, C., Dragani, W., Meyerjuergens, J., Giesecke, R., Cucco, A., Fenco, H. 2023. General circulation and tidal wave propagation along the Beagle Channel. Journal of Marine Systems, 240: 103889. https://doi.org/10.1016/j.jmarsys.2023.103889

Miquel, J.-C., Gasser, B. Martín, J., Marec, C., Babin, M., Fortier, L., Forest, A. (2015). Downward particle flux and carbon export in the Beaufort Sea, Arctic Ocean; the role of zooplankton. Biogeosciences, 12: 5103-5117. https://doi.org/10.5194/bg-12-5103-2015

Mortlock, R. A. and Froelich, P. N. (1989). A simple method for the rapid determination of biogenic opal in pelagic marine sediments. Deep Sea Research Part A. Oceanographic Research Papers, 36(9), 1415-1426. https://doi.org/10.1016/0198-0149(89)90092-7

Müller, P.J. and Schneider, R. (1993). An automated leaching method for the determination of opal in sediments and particulate matter. Deep Sea Research, Part I,

Oceanographic Research Papers, 40(3), 425−444. https://doi.org/10.1016/0967-0637(93)90140-X

Nguyen, T.T.H., Zakem, E.J., Ebrahimi, A., Schwartzman, J., Caglar, T., Amarnath, K., Alcolombri, U., Peaudecerf, F.J., Hwa, T., Stocker, R., Cordero, O.X., Levine, N.M. (2022). Microbes contribute to setting the ocean carbon flux by altering the fate of sinking particulates. Nat. Commun. 13, 1–9. https://doi.org/10.1038/s41467-022-29297-2

Omand, M. M., Govindarajan, R., He, J. and Mahadevan, A. (2020). Sinking flux of particulate organic matter in the oceans: Sensitivity to particle characteristics. Sci. Rep. 10, 5582. https://doi.org/10.1038/s41598-020-60424-5

Pagès, F., Martín, J., Palanques, A., Puig, P., Gili, J.M. (2007). High occurrence of the elasipodid holothurian *Penilpidia ludwigi* (von Marenzeller, 1893) in bathyal sediment traps moored in a western Mediterranean submarine canyon. Deep Sea Research Part I Oceanographic Research Papers 54, 2170-2180. https://doi.org/10.1016/j.dsr.2007.09.002

Paredes, M. A., and Montecino, V. (2011). Size diversity as an expression of phytoplankton community structure and the identification of its patterns on the scale of fjords and channels. Continental Shelf Research, 31(3-4), 272-281. https://doi.org/10.1016/j.csr.2010.07.012

Pérez-Barros, P., Romero, M. C., Calcagno, J. A., and Lovrich, G. A. (2010). Similar feeding habits of two morphs of *Munida gregaria* (Decapoda) evidence the lack of trophic polymorphism. Revista de biología marina y oceanografía, 45(3), 461-470. http://dx.doi.org/10.4067/S0718-19572010000300011

Rember, R. and Trefry, J. (2005). Sediment and organic carbon focusing in the Shelikof Strait, Alaska. Marine geology, 224(1-4), 83-101. https://doi.org/10.1016/j.margeo.2005.06.036

Riccialdelli, L., Newsome, S. D., Fogel, M. L., and Fernández, D. A. (2017). Trophic interactions and food web structure of a subantarctic marine food web in the Beagle Channel: Bahía Lapataia, Argentina. Polar Biology, 40(4), 807-821. https://doi.org/10.1007/s00300-016-2007-x

Rodríguez-Flórez, C.N. Paczkowska, J., Martín, J., Gil, M.N., Flores-Melo, X., Malits, A. J., (2023). Terrigenous DOM input and nutrient-light-limited conditions on the winter microbial food web of the Argentinian Beagle Channel. J. Mar. Syst. https://doi.org/10.1016/j.jmarsys.2023.103860

Sarmiento, J.L., 2013. Ocean Biogeochemical Dynamics. Princeton University Press. 495 pp. https://doi.org/10.1515/9781400849079

Schlitzer, R. (2021). Ocean Data View. https://odv.awi.de

Schloss, I.R., Pizarro, G., Cadaillon, A.M., Giesecke, R., Hernando, M.P., Almandoz, G.O., Latorre, M.P., Malits, A., Flores-Melo, X., Saravia, L.A., Martín, J., Guzmán, L., Iachetti, C.M., Ruiz, C. (2023). Alexandrium catenella dynamics and paralytic shellfish toxins distribution along the Beagle Channel (southern Patagonia). J. Mar. Syst. 239. https://doi.org/10.1016/j.jmarsys.2022.103856

Sejr, M.K., Krause-Jensen, D., Dalsgaard, T., Ruiz-Halpern, S., Duarte, C.M., Middelboe, M., Glud, R.N., Bendtsen, J., Balsby, T.J.S., Rysgaard, S. (2014). Seasonal dynamics of autotrophic and heterotrophic plankton metabolism and PCO2 in a subarctic Greenland fjord. Limnol. Oceanogr. 59, 1764–1778. https://doi.org/10.4319/lo.2014.59.5.1764

Steinberg, D. K., and Landry, M. R. (2017). Zooplankton and the ocean carbon cycle. Annual review of marine science, 9, 413-444. https://doi.org/10.1146/annurev-marine-010814-015924

Sunda, W.G. and Huntsman, S.A., 1997. Interrelated influence of iron, light and cell size on marine phytoplankton growth. Nature, 390(6658), pp. 389-392. https://doi.org/10.1038/37093

Tas, S., and Hernández-Becerril, D. U. (2017). Diversity and distribution of the planktonic diatom genus Chaetoceros (Bacillariophyceae) in the Golden Horn Estuary (Sea of Marmara). Diatom research, 32(3), 309-323. https://doi.org/10.1080/0269249X.2017.1360800

Torres, R., Pantoja, S., Harada, N., González, H.E., Daneri, G., Frangopulos, M., Rutllant, J.A., Duarte, C.M., Rúiz-Halpern, S., Mayol, E., Fukasawa, M. (2011). Air-sea CO2 fluxes along the coast of Chile: From CO2 outgassing in central northern upwelling waters to CO2 uptake in southern Patagonian fjords. J. Geophys. Res. Ocean. 116, 1–17. https://doi.org/10.1029/2010JC006344

Turner, J.T. (2015). Zooplankton fecal pellets, marine snow, phytodetritus and the ocean's biological pump. Progress in Oceanography 130: 205-248. https://doi.org/10.1016/j.pocean.2014.08.005

Utermöhl, H. (1958). Zur Vervollkommnung der quantitativen Phytoplankton. Methodik. Mitt. Int. Ver. Theor. Angew. Limnol. 9,1–39

Varela, M., Prego, R., Pazos, Y. (2004). Vertical biogenic particle flux in a western Galician ria (NW Iberian Peninsula). Mar. Ecol. Prog. Ser. 269, 17–32. https://doi.org/10.3354/meps269017

Acknowledgments

Declaration of interests

☒The authors declare that they have no known competing financial interests or personal relationships that could have appeared to influence the work reported in this paper.

☐The authors declare the following financial interests/personal relationships which may be considered as potential competing interests:

Highlights

- The presence of ballast matter in glacier-influenced sectors enhances carbon flux year-round.
- Biogenic fluxes tightly coupled with local production dominate the non-glacier sector
- Here, maximum downward carbon flux occurs during the spring bloom.
- Nano and picophytoplankton nourish fall and winter carbon exports.